d^2 and d^8 Quadrate Energy Levels Including Spin–Orbit Perturbation

by Jayarama R. Perumareddi

Department of Chemistry, Florida Atlantic University, Boca Raton, Florida 33432 *(Received June 7, 1972)*

Starting from strong-field octahedral representation, the symmetry adapted quadrate wave functions are derived in both coordinate and spin space for d^2 and d^8 electronic configurations. The corresponding energy matrices are constructed as parametrically dependent on ligand field, electron correlation, and spin–orbit interaction perturbations in the coupling scheme in which the spin–orbit perturbation is applied last. The energy diagrams displaying the splittings of the cubic energy levels by the additive axial part of the quadrate ligand field and further by the spin–orbit perturbations are obtained by considering octahedral d^8 configuration as an example. The importance of full configuration interaction on the quadrate splittings of the cubic energy levels is emphasized. Applications of our energy equations to optical spectral and magnetic studies on quadrately distorted or substituted octahedral, quadrately distorted tetrahedral, and five-coordinate square pyramidal systems, of d^2 and d^8 electronic configurations, are pointed out.

I. Introduction

The few attempts that have been made so far in interpreting the electronic spectra of quadrate (tetragonal) nickel(II) complexes made use of energy levels with no spin–orbit perturbation, and either with complete or partial neglect of configuration interaction.[1] Treatment of octahedral nickel(II) complexes with full configuration interaction and spin–orbit perturbation in the past[2] gave rise to a better understanding of their electronic structures. Inclusion of configuration interaction is very important in that it may alter the energies considerably and in some instances even affect the assignments. Spin–orbit interaction, though it acts as a minor perturbation in the case of the early members of the 3d transition series elements, can be dominant for the later members of the series. It is certainly necessary to include spin–orbit perturbation for meaningful studies on systems involving elements of 4d and 5d transition series.

The purpose of this investigation is to derive the energy levels of d^2 and d^8 electronic configurations immersed in quadrate ligand fields including spin–orbit perturbation with complete configuration interaction and interpret the electronic spectra of appropriate compounds. The present report is concerned with the development of the underlying theory. Applications of the theory to optical spectra and other experimental data will be described in future papers. The appropriate compounds of d^2 and d^8 electronic configurations that can be studied by the theory developed here are the tetragonally distorted or substituted octahedral and tetrahedral complexes and the five-coordinate square pyramidal systems. The tetragonally substituted octahedral complexes include the mono- and the trans disubstituted octahedral systems. The cis disubstituted octahedral complexes can also be treated by the same theory if it is assumed that the ligand fields of trans ligand pairs can be averaged.[3]

II. Theory

Octahedral Orientation. In the systems for which the theory is developed here, the additive axial ligand field acts as a minor perturbation relative to the major cubic ligand field so that these systems can be treated as slightly distorted cubic field complexes. In other words, we shall use the two electron cubic wave functions as the basis set which will then be decomposed properly to correspond to the symmetry adapted functions of quadrate symmetry. The decomposition of the cubic functions relative to the representations of quadrate symmetry is given in Table I.

Coupling Scheme. We utilize the coupling scheme in which the spin–orbit perturbation is applied last. If V_C, V_a, $\Sigma_{j>i}e^2/r_{ij}$, and $\Sigma_i\xi(r_i)\vec{l}_i\cdot\vec{s}_i$ denote, respectively, the perturbations due to the cubic ligand field, axial ligand field, electron correlation, and spin–orbit interaction, the sequence[4] in which these perturbations are applied is as follows

$$V_C > \sum_{j>i} e^2/r_{ij} > V_a > \sum_i \xi(r_i)\vec{l}_i\cdot\vec{s}_i$$

Wave Functions. The procedure of fabricating symmetry adapted two-electron cubic wave functions in coordinate space is well known.[5] Once these are ob-

(1) (a) See for a review of these, N. S. Hush and R. J. M. Hobbs, "Progress in Inorganic Chemistry," Vol. 10, F. A. Cotton, Ed., Interscience Publishers, New York, 1968. See also (b) C. W. Reimann, *J. Phys. Chem.*, **74**, 561 (1970); (c) R. L. Chiang and R. S. Drago, *Inorg. Chem.*, **10**, 453 (1971), and references therein.

(2) A. D. Liehr and C. J. Ballhausen, *Ann. Phys.*, **6**, 134 (1959).

(3) (a) R. Krishnamurthy, W. B. Schaap, and J. R. Perumareddi, *Inorg. Chem.*, **6**, 1338 (1967); (b) J. R. Perumareddi, *Coord. Chem. Rev.*, **4**, 73 (1969).

(4) For a review and importance of other coupling schemes possible for low-symmetry ligand fields, read (a) J. R. Perumareddi, *J. Phys. Chem.*, **71**, 3144 (1967); (b) J. R. Perumareddi and A. D. Liehr, Abstracts, Symposium on Molecular Structure and Spectroscopy, Columbus, Ohio, June 14–19, 1965; (c) J. R. Perumareddi, to be submitted for publication.

(5) See, for instance, C. J. Ballhausen, "Introduction to Ligand Field Theory," McGraw-Hill, New York, N. Y., 1962.

Table I: Decomposition of Cubic Representations Relative to Quadrate Symmetry

Cubic	Quadrate	Cubic	Quadrate
$A_{1g}{}^C$	$A_{1g}{}^Q$	$T_{1gb}{}^C$	$E_{ga}{}^Q$
$A_{2g}{}^C$	$B_{1g}{}^Q$	$T_{1gc}{}^C$	$E_{gb}{}^Q$
$E_{ga}{}^C$	$A_{1g}{}^Q$	$T_{2ga}{}^C$	$B_{2g}{}^Q$
$E_{gb}{}^C$	$B_{1g}{}^Q$	$T_{2gb}{}^C$	$E_{ga}{}^Q$
$T_{1ga}{}^C$	$A_{2g}{}^Q$	$T_{2gc}{}^C$	$E_{gb}{}^Q$

tained, they are decomposed to quadrate functions according to the Table I. The next step is to make these functions symmetry adapted including spin space. It should be noted that the spin-singlet functions are symmetry adapted both in coordinate and spin space to begin with. We need only make the spin-triplet functions spin oriented. This is done by first studying the symmetry transformation properties of spin functions. If α and β represent the one-electron spin states, their transformation properties can be obtained by the substitution of angular values into the spinor array of Goldstein[6] after the angles are determined by identifying the transformation matrix of the symmetry operation with the Eulerian matrix.[6] The two-electron spin functions properly transforming as the cubic and quadrate representations can then be constructed by examining the transformation properties of the two-electron spin "product" functions. The spin functions so constructed and their symmetry transformation properties are given in Table II which also includes the transformation properties of orbital representations. The inclusion of spin space is then achieved by appropriately combining these spin functions with the orbital functions resulting in quadrate functions which are again made to transform in exactly the same way as the symmetry transformations of quadrate representations shown in Table II. The two-electron wave functions which are symmetry adapted both in coordinate and spin space[7] derived by this procedure are given in Table III. The corresponding eight-electron wave functions can be easily obtained if needed from those listed by considering the two electrons as holes.

Energy Matrices. The various perturbations can be parametrized as usual.[4] Thus, the ligand field gives rise to a cubic Dq and axial Ds, Dt parameters, the electron correlation yields the A, B, C parameters, and the spin-orbit perturbation results in a one-electron spin-orbit coupling constant parameter ζ.

The secular determinants obtained as a function of these parameters with the use of the wave functions of Table III are given in Tables IVa to e. The cubic ligand field (Dq) is completely diagonalized, as it should be, in these energy matrices. The electron correlation (A, B, C) and the axial ligand field (Ds, Dt) are diagonal, respectively, in the cubic quantum number $\{X_j{}^C\}$ and quadrate quantum number $\{X_j{}^Q\}$.

Table II: Symmetry Transformation Properties of Quadrate Oriented Cubic Orbital and Spin Functions

Function	Representation: Cubic	Representation: Quadrate	Symmetry operation: $C_4(z)$	Symmetry operation: $C_2(y)$	Symmetry operation: $C_3(z')$
z	t_{1ua}	a_2	t_{1ua}	$-t_{1ua}$	t_{1ub}
y	t_{1ub}	e_a	t_{1uc}	t_{1ub}	t_{1uc}
x	t_{1uc}	e_b	$-t_{1ub}$	$-t_{1uc}$	t_{1ua}
xy	t_{2ga}	b_2	$-t_{2ga}$	$-t_{2ga}$	t_{2gb}
zx	t_{2gb}	e_a	$-t_{2gc}$	t_{2gb}	t_{2gc}
yz	t_{2gc}	e_b	t_{2gb}	$-t_{2gc}$	t_{2ga}
z^2	e_{ga}	a_1	e_{ga}	e_{ga}	$-\frac{1}{2}e_{ga} - \frac{\sqrt{3}}{2}e_{gb}$
$(x^2 - y^2)$	e_{gb}	b_1	$-e_{gb}$	e_{gb}	$-\frac{1}{2}e_{gb} + \frac{\sqrt{3}}{2}e_{ga}$
$(\alpha\beta - \beta\alpha)/\sqrt{2}$	a_1	a_1	a_1	a_1	a_1
$(\alpha\beta + \beta\alpha)/\sqrt{2}$	t_{1a}	a_2	t_{1a}	$-t_{1a}$	t_{1b}
$i(\alpha\alpha + \beta\beta)/\sqrt{2}$	t_{1b}	e_a	t_{1c}	t_{1b}	t_{1c}
$-(\alpha\alpha - \beta\beta)/\sqrt{2}$	t_{1c}	e_b	$-t_{1b}$	$-t_{1c}$	t_{1a}

The spin-orbit interaction (ζ), of course, is diagonal only in the double group quadrate quantum number $\{\Gamma_j{}^Q\}$. It should be noted that in the limit of zero spin-orbit and axial ligand field perturbations, these energy matrices become identical with the cubic d^2 energy matrices of Tanabe and Sugano[8] within phases. The correctness of our quadrate energy matrices had been checked by directly calculating all the matrix elements from the corresponding energy matrices of the other coupling schemes possible and the unitary transformation matrices connecting these coupling schemes with the coupling scheme used in this report.

The quadrate energy matrices of d^8 configuration are obtained simply by changing the sign of Dt, Ds, and ζ. The constant additive energy term in the diagonal elements, $27A - 42B + 21C$, only shifts the d^8 energies but does not affect the energy differences. With the appropriate sign for ζ, the energy equations listed here are applicable to quadrately distorted or substituted octahedral d^8 and quadrately distorted tetrahedral d^8

(6) H. Goldstein, "Classical Mechanics," Addison-Wesley, Cambridge, Mass., 1951.

(7) The symmetry adapted wave functions with and without spin space, respectively, are given the Bethe's Γ_i (i = 1 to 5) and Mulliken's X_j ($X_j{}^C$ = A_1, A_2, E, T_1, T_2 and $X_j{}^Q$ = A_1, A_2, B_1, B_2, and E) classifications. It should be noted that although the energy levels in the diagrams have superscripts Q and C to denote, respectively, the quadrate symmetry designation and cubic parentage, these superscripts have been omitted in the main text for convenience. Similarly quadrate levels have been written variously with and without a g subscript in this report. Strictly speaking, if the complex is noncentrosymmetric (*e.g.*, C_{4v}), the quadrate levels should not have the g subscript. The g subscript should be retained for the quadrate representations of a centrosymmetric complex (*e.g.*, D_{4h}).

(8) (a) Y. Tanabe and S. Sugano, *J. Phys. Soc. Jap.*, 9, 753 (1954); (b) see also S. Sugano, Y. Tanabe, and H. Kamimura, "Multiplets of Transition-Metal Ions in Crystals," Academic Press, New York, N. Y., 1970.

Table III: Two-Electron Spin-Adapted Quadrate Wave Functions

$[\Psi_0 = (\alpha\beta + \beta\alpha)/\sqrt{2},\ \Psi_1 = i(\alpha\alpha + \beta\beta)/\sqrt{2},\ \Psi_{-1} = -(\alpha\alpha - \beta\beta)/\sqrt{2}]$

Γ_1 Representation

$$|1\rangle = {}^3A_{2g}[{}^3T_{1g}(t_{2g}^2)] = |(zx)(yz)|\Psi_0$$

$$|2\rangle = {}^3E_g[{}^3T_{1g}(t_{2g}^2)] = \frac{1}{\sqrt{2}}[|(yz)(xy)|\Psi_1 + |(xy)(zx)|\Psi_{-1}]$$

$$|3\rangle = {}^3E_g[{}^3T_{2g}(t_{2g}e_g)] = \frac{1}{\sqrt{2}}\left\{\left[-\frac{1}{2}|(zx)(z^2)| - \frac{\sqrt{3}}{2}|(zx)(x^2-y^2)|\right]\Psi_1 - \left[-\frac{1}{2}|(yz)(z^2)| + \frac{\sqrt{3}}{2}|(yz)(x^2-y^2)|\right]\Psi_{-1}\right\}$$

$$|4\rangle = {}^3A_{2g}[{}^3T_{1g}(t_{2g}e_g)] = |(xy)(x^2-y^2)|\Psi_0$$

$$|5\rangle = {}^3E_g[{}^3T_{1g}(t_{2g}e_g)] = \frac{1}{\sqrt{2}}\left\{\left[-\frac{1}{2}|(zx)(x^2-y^2)| + \frac{\sqrt{3}}{2}|(zx)(z^2)|\right]\Psi_1 + \left[-\frac{1}{2}|(yz)(x^2-y^2)| - \frac{\sqrt{3}}{2}|(yz)(z^2)|\right]\Psi_{-1}\right\}$$

$$|6\rangle = {}^1A_{1g}[{}^1A_{1g}(t_{2g}^2)] = \frac{1}{\sqrt{3}}[|(xy)(xy)| + |(zx)(zx)| + |(yz)(yz)|](\alpha\beta - \beta\alpha)/\sqrt{2}$$

$$|7\rangle = {}^1A_{1g}[{}^1E_g(t_{2g}^2)] = \frac{1}{\sqrt{6}}[-2|(xy)(xy)| + |(zx)(zx)| + |(yz)(yz)|](\alpha\beta - \beta\alpha)/\sqrt{2}$$

$$|8\rangle = {}^1A_{1g}[{}^1A_{1g}(e_g^2)] = \frac{1}{\sqrt{2}}[|(z^2)(z^2)| + |(x^2-y^2)(x^2-y^2)|](\alpha\beta - \beta\alpha)/\sqrt{2}$$

$$|9\rangle = {}^1A_{1g}[{}^1E_g(e_g^2)] = \frac{1}{\sqrt{2}}[|(z^2)(z^2)| - |(x^2-y^2)(x^2-y^2)|](\alpha\beta - \beta\alpha)/\sqrt{2}$$

Γ_2 Representation

$$|1\rangle = {}^3E_g[{}^3T_{1g}(t_{2g}^2)] = \frac{1}{\sqrt{2}}[|(yz)(xy)|\Psi_{-1} - |(xy)(zx)|\Psi_1]$$

$$|2\rangle = {}^3E_g[{}^3T_{2g}(t_{2g}e_g)] = \frac{1}{\sqrt{2}}\left\{\left[-\frac{1}{2}|(zx)(z^2)| - \frac{\sqrt{3}}{2}|(zx)(x^2-y^2)|\right]\Psi_{-1} + \left[-\frac{1}{2}|(yz)(z^2)| + \frac{\sqrt{3}}{2}|(yz)(x^2-y^2)|\right]\Psi_1\right\}$$

$$|3\rangle = {}^3E_g[{}^3T_{1g}(t_{2g}e_g)] = \frac{1}{\sqrt{2}}\left\{\left[-\frac{1}{2}|(zx)(x^2-y^2)| + \frac{\sqrt{3}}{2}|(zx)(z^2)|\right]\Psi_{-1} - \left[-\frac{1}{2}|(yz)(x^2-y^2)| - \frac{\sqrt{3}}{2}|(yz)(z^2)|\right]\Psi_1\right\}$$

$$|4\rangle = {}^1A_{2g}[{}^1T_{1g}(t_{2g}e_g)] = |(xy)(x^2-y^2)|(\alpha\beta - \beta\alpha)/\sqrt{2}$$

Γ_3 Representation

$$|1\rangle = {}^3E_g[{}^3T_{1g}(t_{2g}^2)] = \frac{1}{\sqrt{2}}[|(yz)(xy)|\Psi_1 - |(xy)(zx)|\Psi_{-1}]$$

$$|2\rangle = {}^3B_{2g}[{}^3T_{2g}(t_{2g}e_g)] = |(xy)(z^2)|\Psi_0$$

$$|3\rangle = {}^3E_g[{}^3T_{2g}(t_{2g}e_g)] = \frac{1}{\sqrt{2}}\left\{\left[-\frac{1}{2}|(zx)(z^2)| - \frac{\sqrt{3}}{2}|(zx)(x^2-y^2)|\right]\Psi_1 + \left[-\frac{1}{2}|(yz)(z^2)| + \frac{\sqrt{3}}{2}|(yz)(x^2-y^2)|\right]\Psi_{-1}\right\}$$

$$|4\rangle = {}^3E_g[{}^3T_{1g}(t_{2g}e_g)] = \frac{1}{\sqrt{2}}\left\{\left[-\frac{1}{2}|(zx)(x^2-y^2)| + \frac{\sqrt{3}}{2}|(zx)(z^2)|\right]\Psi_1 - \left[-\frac{1}{2}|(yz)(x^2-y^2)| - \frac{\sqrt{3}}{2}|(yz)(z^2)|\right]\Psi_{-1}\right\}$$

$$|5\rangle = {}^1B_{1g}[{}^1E_g(t_{2g}^2)] = \frac{1}{\sqrt{2}}[|(zx)(zx)| - |(yz)(yz)|](\alpha\beta - \beta\alpha)/\sqrt{2}$$

$$|6\rangle = {}^1B_{1g}[{}^1E_g(e_g^2)] = -\frac{1}{\sqrt{2}}[|(z^2)(x^2-y^2)| + |(x^2-y^2)(z^2)|](\alpha\beta - \beta\alpha)/\sqrt{2}$$

Table III (*Continued*)

Γ_4 Representation

$$|1\rangle = {}^3E_g[{}^3T_{1g}(t_{2g}^2)] = \frac{1}{\sqrt{2}}[|(yz)(xy)|\Psi_{-1} + |(xy)(zx)|\Psi_1]$$

$$|2\rangle = {}^3E_g[{}^3T_{2g}(t_{2g}e_g)] = \frac{1}{\sqrt{2}}\left\{\left[-\frac{1}{2}|(zx)(z^2)| - \frac{\sqrt{3}}{2}|(zx)(x^2-y^2)|\right]\Psi_{-1} - \left[-\frac{1}{2}|(yz)(z^2)| + \frac{\sqrt{3}}{2}|(yz)(x^2-y^2)|\right]\Psi_1\right\}$$

$$|3\rangle = {}^3E_g[{}^3T_{1g}(t_{2g}e_g)] = \frac{1}{\sqrt{2}}\left\{\left[-\frac{1}{2}|(zx)(x^2-y^2)| + \frac{\sqrt{3}}{2}|(zx)(z^2)|\right]\Psi_{-1} + \left[-\frac{1}{2}|(yz)(x^2-y^2)| - \frac{\sqrt{3}}{2}|(yz)(z^2)|\right]\Psi_1\right\}$$

$$|4\rangle = {}^3B_{1g}[{}^3A_{2g}(e_g^2)] = |(z^2)(x^2-y^2)|\Psi_0$$

$$|5\rangle = {}^1B_{2g}[{}^1T_{2g}(t_{2g}^2)] = \frac{1}{\sqrt{2}}[|(zx)(yz)| + |(yz)(zx)|](\alpha\beta - \beta\alpha)/\sqrt{2}$$

$$|6\rangle = {}^1B_{2g}[{}^1T_{2g}(t_{2g}e_g)] = |(xy)(z^2)|(\alpha\beta - \beta\alpha)/\sqrt{2}$$

$\Gamma_{5a,b}$ Representation

$$|1\rangle = {}^3A_{2g}[{}^3T_{1g}(t_{2g}^2)] = |(zx)(yz)|\Psi_{-1}, - |(zx)(yz)|\Psi_1$$

$$|2\rangle = {}^3E_g[{}^3T_{1g}(t_{2g}^2)] = |(xy)(zx)|\Psi_0, - |(yz)(xy)|\Psi_0$$

$$|3\rangle = {}^3B_{2g}[{}^3T_{2g}(t_{2g}e_g)] = |(xy)(z^2)|\Psi_{-1}, |(xy)(z^2)|\Psi_1$$

$$|4\rangle = {}^3E_g[{}^3T_{2g}(t_{2g}e_g)] = -\left[-\frac{1}{2}|(yz)(z^2)| + \frac{\sqrt{3}}{2}|(yz)(x^2-y^2)|\right]\Psi_0, - \left[-\frac{1}{2}|(zx)(z^2)| - \frac{\sqrt{3}}{2}|(zx)(x^2-y^2)|\right]\Psi_0$$

$$|5\rangle = {}^3A_{2g}[{}^3T_{1g}(t_{2g}e_g)] = |(xy)(x^2-y^2)|\Psi_{-1}, - |(xy)(x^2-y^2)|\Psi_1$$

$$|6\rangle = {}^3E_g[{}^3T_{1g}(t_{2g}e_g)] = \left[-\frac{1}{2}|(yz)(x^2-y^2)| - \frac{\sqrt{3}}{2}|(yz)(z^2)|\right]\Psi_0, \left[\frac{1}{2}|(zx)(x^2-y^2)| - \frac{\sqrt{3}}{2}|(zx)(z^2)|\right]\Psi_0$$

$$|7\rangle = {}^3B_{1g}[{}^3A_{2g}(e_g^2)] = |(z^2)(x^2-y^2)|\Psi_1, - |(z^2)(x^2-y^2)|\Psi_{-1}$$

$$|8\rangle = {}^1E_g[{}^1T_{2g}(t_{2g}^2)] = \frac{1}{\sqrt{2}}[|(yz)(xy)| + |(xy)(yz)|](\alpha\beta - \beta\alpha)/\sqrt{2}, \frac{1}{\sqrt{2}}[|(xy)(zx)| + |(zx)(xy)|](\alpha\beta - \beta\alpha)/\sqrt{2}$$

$$|9\rangle = {}^1E_g[{}^1T_{1g}(t_{2g}e_g)] = \left[-\frac{1}{2}|(zx)(x^2-y^2)| + \frac{\sqrt{3}}{2}|(zx)(z^2)|\right](\alpha\beta - \beta\alpha)/\sqrt{2}, \left[-\frac{1}{2}|(yz)(x^2-y^2)| - \frac{\sqrt{3}}{2}|(yz)(z^2)|\right](\alpha\beta - \beta\alpha)/\sqrt{2}$$

$$|10\rangle = {}^1E_g[{}^1T_{2g}(t_{2g}e_g)] = \left[-\frac{1}{2}|(zx)(z^2)| - \frac{\sqrt{3}}{2}|(zx)(x^2-y^2)|\right](\alpha\beta - \beta\alpha)/\sqrt{2}, \left[-\frac{1}{2}|(yz)(z^2)| + \frac{\sqrt{3}}{2}|(yz)(x^2-y^2)|\right](\alpha\beta - \beta\alpha)/\sqrt{2}$$

systems and by changing the sign of Dq, they will be applicable to quadrately distorted or substituted octahedral d^8 and quadrately distorted tetrahedral d^2 systems. Similarly the d^2 energy matrices and the d^8 energy matrices obtained by changing the sign of ζ, Dq, Dt, and Ds can also be utilized in studying the electronic structures of the corresponding five-coordinate square pyramidal systems once the Dt and Ds are considered as symmetry parameters.[9]

Energy Diagrams. The splitting of cubic levels by the additive axial ligand field perturbation of quadrate symmetry in the limit of zero spin–orbit interaction[10] is shown in Figure 1 by considering octahedral d^8 configuration as an example. A B value of 800 cm^{-1} is chosen in this diagram to represent a series of octahedral

(9) (a) K. G. Caulton, *Inorg. Chem.*, **7**, 392 (1968); (b) see also J. R. Perumareddi, *J. Phys. Chem.*, **71**, 3155 (1967).

(10) In the limit of zero spin–orbit interaction, with the exception of ^3E_g, ^1E_g which are 3×3 matrices and $^1A_{1g}$ which is a 4×4 matrix, all other levels are either single ($^3B_{1g}$, $^3B_{2g}$, $^1A_{2g}$) or at the most 2×2 matrices ($^3A_{2g}$, $^1B_{1g}$, $^1B_{2g}$). The solutions of 2×2 secular determinants yield the energy equations: $^3A_{2g} = (-3Dq - Ds - 3Dt - {}^1/_2B) \pm {}^1/_2[(10Dq - 6Ds + 10Dt + 9B)^2 + 144B^2]^{1/2}$, $^1B_{1g} = (2Dq + Ds - {}^1/_2Dt + {}^1/_2B + 2C) \pm {}^1/_2[(20Dq - 2Ds + 15Dt - B)^2 + 48B^2]^{1/2}$, and $^1B_{2g} = (-3Dq + Ds - {}^1/_2Dt + {}^1/_2B + 2C) \pm {}^1/_2[(10Dq - 2Ds + 15Dt - B)^2 + 48B^2]^{1/2}$.

Table IVa: Quadrate Energy Matrices of d^2 Electronic Configuration, Γ_1 Representation

Γ_1	$^3A_{2g}[^3T_{1g}(t_{2g}^2)]$	$^3E_g[^3T_{1g}(t_{2g}^2)]$	$^3E_g[^3T_{2g}(t_{2g}e_g)]$	$^3A_{2g}[^3T_{1g}(t_{2g}e_g)]$	$^3E_g[^3T_{1g}(t_{2g}e_g)]$	$^1A_{1g}[^1A_{1g}(t_{2g}^2)]$	$^1A_{1g}[^1E_g(t_{2g}^2)]$	$^1A_{1g}[^1A_{1g}(e_g^2)]$	$^1A_{1g}[^1E_g(e_g^2)]$
$^3A_{2g}[^3T_{1g}(t_{2g}^2)]$	$-8Dq + 2Ds - 8Dt + A - 5B$	$\frac{\sqrt{2}}{2}\zeta$	$-\frac{\sqrt{6}}{2}\zeta$	$-6B$	$\frac{\sqrt{2}}{2}\zeta$	$-i\frac{\sqrt{6}}{3}\zeta$	$-i\frac{\sqrt{3}}{3}\zeta$	0	0
$^3E_g[^3T_{1g}(t_{2g}^2)]$		$-8Dq - Ds - 3Dt + A - 5B + \frac{1}{2}\zeta$	$\frac{\sqrt{3}}{2}\zeta$	$\frac{\sqrt{2}}{2}\zeta$	$-6B + \frac{1}{2}\zeta$	$-i\frac{2\sqrt{3}}{3}\zeta$	$i\frac{\sqrt{6}}{6}\zeta$	0	0
$^3E_g[^3T_{2g}(t_{2g}e_g)]$			$2Dq - \frac{7}{4}Dt + A - 8B + \frac{1}{4}\zeta$	$-\frac{\sqrt{6}}{4}\zeta$	$-\frac{\sqrt{3}}{4}(4Ds + 5Dt) + \frac{\sqrt{3}}{4}\zeta$	0	0	0	$-i\frac{\sqrt{6}}{2}\zeta$
$^3A_{2g}[^3T_{1g}(t_{2g}e_g)]$				$2Dq - 4Ds + 2Dt + A + 4B$	$-\frac{\sqrt{2}}{4}\zeta$	$i\frac{\sqrt{6}}{3}\zeta$	$-i\frac{2\sqrt{3}}{3}\zeta$	$i\zeta$	$-i\zeta$
$^3E_g[^3T_{1g}(t_{2g}e_g)]$					$2Dq + 2Ds + \frac{3}{4}Dt + A + 4B - \frac{1}{4}\zeta$	$i\frac{2\sqrt{3}}{3}\zeta$	$i\frac{\sqrt{6}}{3}\zeta$	$i\sqrt{2}\zeta$	$i\frac{\sqrt{2}}{2}\zeta$
$^1A_{1g}[^1A_{1g}(t_{2g}^2)]$						$-8Dq - \frac{14}{3}Dt + A + 10B + 5C$	$\frac{2\sqrt{2}}{3}(3Ds - 5Dt)$	$\sqrt{6}(2B + C)$	0
$^1A_{1g}[^1E_g(t_{2g}^2)]$							$-8Dq - 2Ds - \frac{4}{3}Dt + A + B + 2C$	0	$-2\sqrt{3}B$
$^1A_{1g}[^1A_{1g}(e_g^2)]$								$12Dq + 7Dt + A + 8B + 4C$	$4Ds + 5Dt$
$^1A_{1g}[^1E_g(e_g^2)]$									$12Dq + 7Dt + A + 2C$

Table IVb: Quadrate Energy Matrices of d^2 Electronic Configuration, Γ_2 Representation

Γ_2	$^3E_g[^3T_{1g}(t_{2g}^2)]$	$^3E_g[^3T_{2g}(t_{2g}e_g)]$	$^3E_g[^3T_{1g}(t_{2g}e_g)]$	$^1A_{2g}[^1T_{1g}(t_{2g}e_g)]$
$^3E_g[^3T_{1g}(t_{2g}^2)]$	$-8Dq - Ds - 3Dt + A - 5B + \frac{1}{2}\zeta$	$\frac{\sqrt{3}}{2}\zeta$	$-6B + \frac{1}{2}\zeta$	$-\frac{i\sqrt{2}}{2}\zeta$
$^3E_g[^3T_{2g}(t_{2g}e_g)]$		$2Dq - \frac{7}{4}Dt + A - 8B + \frac{1}{4}\zeta$	$-\frac{\sqrt{3}}{4}(4Ds + 5Dt) + \frac{\sqrt{3}}{4}\zeta$	$-\frac{i\sqrt{6}}{4}\zeta$
$^3E_g[^3T_{1g}(t_{2g}e_g)]$			$2Dq + 2Ds + \frac{3}{4}Dt + A + 4B - \frac{1}{4}\zeta$	$-\frac{i\sqrt{2}}{4}\zeta$
$^1A_{2g}[^1T_{1g}(t_{2g}e_g)]$				$2Dq - 4Ds + 2Dt + A + 4B + 2C$

Table IVc: Quadrate Energy Matrices of d^2 Electronic Configuration, Γ_3 Representation

Γ_3	$^3E_g[^3T_{1g}(t_{2g}^2)]$	$^3B_{2g}[^3T_{2g}(t_{2g}e_g)]$	$^3E_g[^3T_{2g}(t_{2g}e_g)]$	$^3E_g[^3T_{1g}(t_{2g}e_g)]$	$^1B_{1g}[^1E_g(t_{2g}^2)]$	$^1B_{1g}[^1E_g(e_g^2)]$
$^3E_g[^3T_{1g}(t_{2g}^2)]$	$-8Dq - Ds - 3Dt + A - 5B - \frac{1}{2}\zeta$	$\frac{\sqrt{6}}{2}\zeta$	$-\frac{\sqrt{3}}{2}\zeta$	$-6B - \frac{1}{2}\zeta$	$\frac{i\sqrt{2}}{2}\zeta$	0
$^3B_{2g}[^3T_{2g}(t_{2g}e_g)]$		$2Dq + 7Dt + A - 8B$	$-\frac{\sqrt{2}}{4}\zeta$	$\frac{\sqrt{6}}{4}\zeta$	0	$-i\zeta$
$^3E_g[^3T_{2g}(t_{2g}e_g)]$			$2Dq - \frac{7}{4}Dt + A - 8B - \frac{1}{4}\zeta$	$-\frac{\sqrt{3}}{4}(4Ds + Dt) - \frac{\sqrt{3}}{4}\zeta$	0	$\frac{i\sqrt{2}}{2}\zeta$
$^3E_g[^3T_{1g}(t_{2g}e_g)]$				$2Dq + 2Ds + \frac{3}{4}Dt + A + 4B + \frac{1}{4}\zeta$	$i\sqrt{2}\zeta$	$\frac{i\sqrt{6}}{2}\zeta$
$^1B_{1g}[^1E_g(t_{2g}^2)]$					$-8Dq + 2Ds - 8Dt + A + B + 2C$	$-2\sqrt{3}B$
$^1B_{1g}[^1E_g(e_g^2)]$						$12Dq + 7Dt + A + 2C$

Ni(II) complexes and the theoretical ratio of 4 for C to B is used. Employing fixed values of Dt and κ,[11] the Ds/Dt ratio, the energy levels are plotted as a function of Dq which is varied from 0 to 4000 cm^{-1}. At $Dq = 0$, the levels correspond to those of cylindrical symmetry. It should be noted that for $Dq \sim <125$ cm^{-1}, the $^3E[^3T_{2g}]$ level becomes the ground state.[12] The further splitting of these levels by the additional

Table IVd: Quadrate Energy Matrices of d^2 Electronic Configuration, Γ_4 Representation

Γ_4	$^3E_g[^3T_{1g}(t_{2g}^2)]$	$^3E_g[^3T_{2g}(t_{2g}e_g)]$	$^3E_g[^3T_{1g}(t_{2g}e_g)]$	$^3B_{1g}[^3A_{2g}(e_g^2)]$	$^1B_{2g}[^1T_{2g}(t_{2g}^2)]$	$^1B_{2g}[^1T_{2g}(t_{2g}e_g)]$
$^3E_g[^3T_{1g}(t_{2g}^2)]$	$-8Dq - Ds - 3Dt + A - 5B - \frac{1}{2}\zeta$	$-\frac{\sqrt{3}}{2}\zeta$	$-6B - \frac{1}{2}\zeta$	0	$\frac{i\sqrt{2}}{2}\zeta$	$-\frac{i\sqrt{6}}{2}\zeta$
$^3E_g[^3T_{2g}(t_{2g}e_g)]$		$2Dq - \frac{7}{4}Dt + A - 8B - \frac{1}{4}\zeta$	$-\frac{\sqrt{3}}{4}(4Ds + 5Dt) - \frac{\sqrt{3}}{4}\zeta$	$\sqrt{2}\zeta$	$\frac{i\sqrt{6}}{2}\zeta$	$-\frac{i\sqrt{2}}{4}\zeta$
$^3E_g[^3T_{1g}(t_{2g}e_g)]$			$2Dq + 2Ds + \frac{3}{4}Dt + A + 4B + \frac{1}{4}\zeta$	0	$-\frac{i\sqrt{2}}{2}\zeta$	$\frac{i\sqrt{6}}{4}\zeta$
$^3B_{1g}[^3A_{2g}(e_g^2)]$				$12Dq + 7Dt + A - 8B$	0	$i\zeta$
$^1B_{2g}[^1T_{2g}(t_{2g}^2)]$					$-8Dq + 2Ds - 8Dt + A + B + 2C$	$2\sqrt{3}B$
$^1B_{2g}[^1T_{2g}(t_{2g}e_g)]$						$2Dq + 7Dt + A + 2C$

spin–orbit perturbation (Liehr–Ballhausen diagram) is displayed in Figure 2[13] where once again the energy levels have been plotted for the same set of parameters but with a value of -550 cm^{-1} for the one-electron spin–orbit coupling constant parameter,[14] ζ.

Similar to quadrate d^3 systems,[3,4a] it has been noted before[1,4b,c] (*cf.* also Tables IVc and IVd or Table IVe) that in the case of quadrate d^8 complexes also[15] the difference in energy between the B_2 component of the first cubic band, $^3T_{2g}$, and the B_1 ground state is 10 Dq including configuration interaction. Because of this conclusion, energy diagrams constructed by fixing a value of Dq appropriate to a parent octahedral complex and varying Dt will be convenient in studying the spectral properties of a series of mono and trans disubstituted derivatives of that octahedral complex.[3,9b] Such an energy diagram is shown in Figure 3 for a Dq value of 1075 cm^{-1} which is that of a hexaammine complex. In this diagram, the Dt is varied from $+2000$ to -2000 cm^{-1} and a κ value of 3 is employed. At zero Dt, the levels are those of octahedral symmetry. The energy levels on the positive and negative sides of Dt are applicable to substituted complexes in which the substituting ligands are of weaker and stronger ligand field strength, respectively, than the ligand of the parent octahedral system. The two halves of the diagram with positive and negative Dt also correspond to tetragonally elongated and compressed octahedral systems, respectively. At the extreme end of positive Dt, the sudden change in the trajectory of energy levels is due to change in the ground state[12] from $^3B_1[^3A_{2g}]$ to $^3E[^3T_{2g}]$.

(11) The choice of both Ds and Dt positive for the one-electron parameters corresponds to a pure tetragonal axial compression of the initially cubic system or to a substitution by ligands of stronger ligand field strength along the fourfold axis of the resulting tetragonal system. The choice of both Ds and Dt negative corresponds to a pure axial elongation or to a substitution by ligands of weaker ligand field strength along the fourfold axis. The five-coordinate square pyramidal and the four-coordinate square planar systems can be considered as the semilimiting and limiting cases of the latter choice. The choice of mixed signed magnitudes, *i.e.*, Ds and Dt of opposite signs, corresponds to more complex situations of variable covalency effects. For more discussion on this, see ref 4c.

(12) The change in ground state from $^3B_1[^3A_{2g}]$ to $^3E[^3T_{2g}]$ can take place if $^{35}/_4\,Dt + CI < -10Dq$ where CI is the energy of configuration interaction by which the $^3E[^3T_{2g}]$ level is lowered as compared to its energy in the first-order estimated from the diagonal elements only (see either Table IVd or IVe). If $4Ds + 5Dt + CI < -10Dq - 12B$, where CI is the energy due to configuration interaction by which the $^3A_2[^3T_{1g}(t_{2g}^5e_g^3)]$ level is lowered as compared to its energy without configuration interaction, then the $^3A_2[^3T_{1g}(t_{2g}^5e_g^3)]$ level becomes the ground state (see either Tables IVa and IVd or Table IVe). This situation is identical with the quadrate case of octahedral d^3 (*cf.* ref 9b, 15, 16).

(13) The superscripts on the energy labels in the figure refer to the percentage content of that eigenvector component of the eigenfunction. The various symbols have the following meaning: § = 75 ± 2.5%, ‡ = 70 ± 2.5%, ‡‡ = 65 ± 2.5%, $ = 60 ± 2.5%, ¢ = 55 ± 2.5%, ₱ = 50 ± 2.5%, ¥ = 45 ± 2.5%, # = 40 ± 2.5%, ¥ = 35 ± 2.5%, Đ = 30 ± 2.5%, Ŧ = 25 ± 2.5%, and ₦ = 20 ± 2.5%. No superscript implies greater than 75%.

(14) Although the free ion ζ value of nickel(II) is -666 cm^{-1} [A. D. Liehr, *J. Phys. Chem.*, **67**, 1314 (1963)], the available optical and magnetic studies of nickel(II) complexes show that it is usually reduced to around -550 cm^{-1} in the complexes.

(15) The similarity of d^8 and d^3 configurations in octahedral ligand fields in the limit of zero spin–orbit interaction [see for instance, J. R. Perumareddi, *Z. Naturforsch. B*, **22**, 908 (1967)] extends to quadrate ligand fields also. The quadrate splittings of the (spin) triplet octahedral levels of d^8 are identical with those of the (spin) quartet octahedral levels of d^3. Thus, the quadrate splittings of the three spin-allowed cubic bands in the case of octahedral d^8 are given by $^3T_{2g}(^3B_{2g} - {}^3E_g) = -{}^{35}/_4Dt$, $^3T_{1g}(^3A_{2g} - {}^3E_g) = 6Ds - {}^5/_4Dt$, and $^3T_{1g}(^3A_{2g} - {}^3E_g) = -3Ds + 5Dt$ (*cf.* either Tables IVa and IVc or Table IVe).

Table IVe: Quadrate Energy Matrices of d^2 Electronic Configuration, Γ_5 Representation

Γ_5	$^3A_{2g}[^3T_{1g}(t_{2g}^2)]$	$^3E_g[^3T_{1g}(t_{2g}^2)]$	$^3B_{2g}[^3T_{2g}(t_{2g}e_g)]$	$^3E_g[^3T_{2g}(t_{2g}e_g)]$	$^3A_{2g}[^3T_{1g}(t_{2g}e_g)]$	$^3E_g[^3T_{1g}(t_{2g}e_g)]$	$^3B_{1g}[^3A_{2g}(e_g^2)]$	$^1E_g[^1T_{2g}(t_{2g}^2)]$	$^1E_g[^1T_{1g}(t_{2g}e_g)]$	$^1E_g[^1T_{2g}(t_{2g}e_g)]$
$^3A_{2g}[^3T_{1g}(t_{2g}^2)]$	$-8Dq + 2Ds - 8Dt + A - 5B$	$-\frac{1}{2}\zeta$	0	$\frac{\sqrt{3}}{2}\zeta$	$-6B$	$-\frac{1}{2}\zeta$	0	$\frac{i}{2}\zeta$	$\frac{i}{2}\zeta$	$-\frac{i\sqrt{3}}{2}\zeta$
$^3E_g[^3T_{1g}(t_{2g}^2)]$		$-8Dq - Ds - 3Dt + A - 5B$	$\frac{\sqrt{3}}{2}\zeta$	0	$-\frac{1}{2}\zeta$	$-6B$	0	$\frac{i}{2}\zeta$	$-\frac{i}{2}\zeta$	$-\frac{i\sqrt{3}}{2}\zeta$
$^3B_{2g}[^3T_{2g}(t_{2g}e_g)]$			$2Dq + 7Dt + A - 8B$	$-\frac{1}{4}\zeta$	0	$\frac{\sqrt{3}}{4}\zeta$	$-\zeta$	$-\frac{i\sqrt{3}}{2}\zeta$	$-\frac{i\sqrt{3}}{4}\zeta$	$\frac{i}{4}\zeta$
$^3E_g[^3T_{2g}(t_{2g}e_g)]$				$2Dq - \frac{7}{4}Dt + A - 8B$	$\frac{\sqrt{3}}{4}\zeta$	$-\frac{\sqrt{3}}{4}(4Ds + 5Dt)$	$-\zeta$	$-\frac{i\sqrt{3}}{2}\zeta$	$\frac{i\sqrt{3}}{4}\zeta$	$\frac{i}{4}\zeta$
$^3A_{2g}[^3T_{1g}(t_{2g}e_g)]$					$2Dq - 4Ds + 2Dt + A + 4B$	$\frac{1}{4}\zeta$	0	$-\frac{i}{2}\zeta$	$\frac{i}{4}\zeta$	$\frac{i\sqrt{3}}{4}\zeta$
$^3E_g[^3T_{1g}(t_{2g}e_g)]$						$2Dq + 2Ds + \frac{3}{4}Dt + A + 4B$	0	$-\frac{i}{2}\zeta$	$-\frac{i}{4}\zeta$	$\frac{i\sqrt{3}}{4}\zeta$
$^3B_{1g}[^3A_{2g}(e_g^2)]$							$12Dq + 7Dt + A - 8B$	0	0	$i\zeta$
$^1E_g[^1T_{2g}(t_{2g}^2)]$								$-8Dq - Ds - 3Dt + A + B + 2C$	0	$2\sqrt{3}B$
$^1E_g[^1T_{1g}(t_{2g}e_g)]$									$2Dq + 2Ds + \frac{3}{4}Dt + A + +4B + 2C$	$-\frac{\sqrt{3}}{4}(4Ds + 5Dt)$
$^1E_g[^1T_{2g}(t_{2g}e_g)]$										$2Dq - \frac{7}{4}Dt$ $A + 2C$

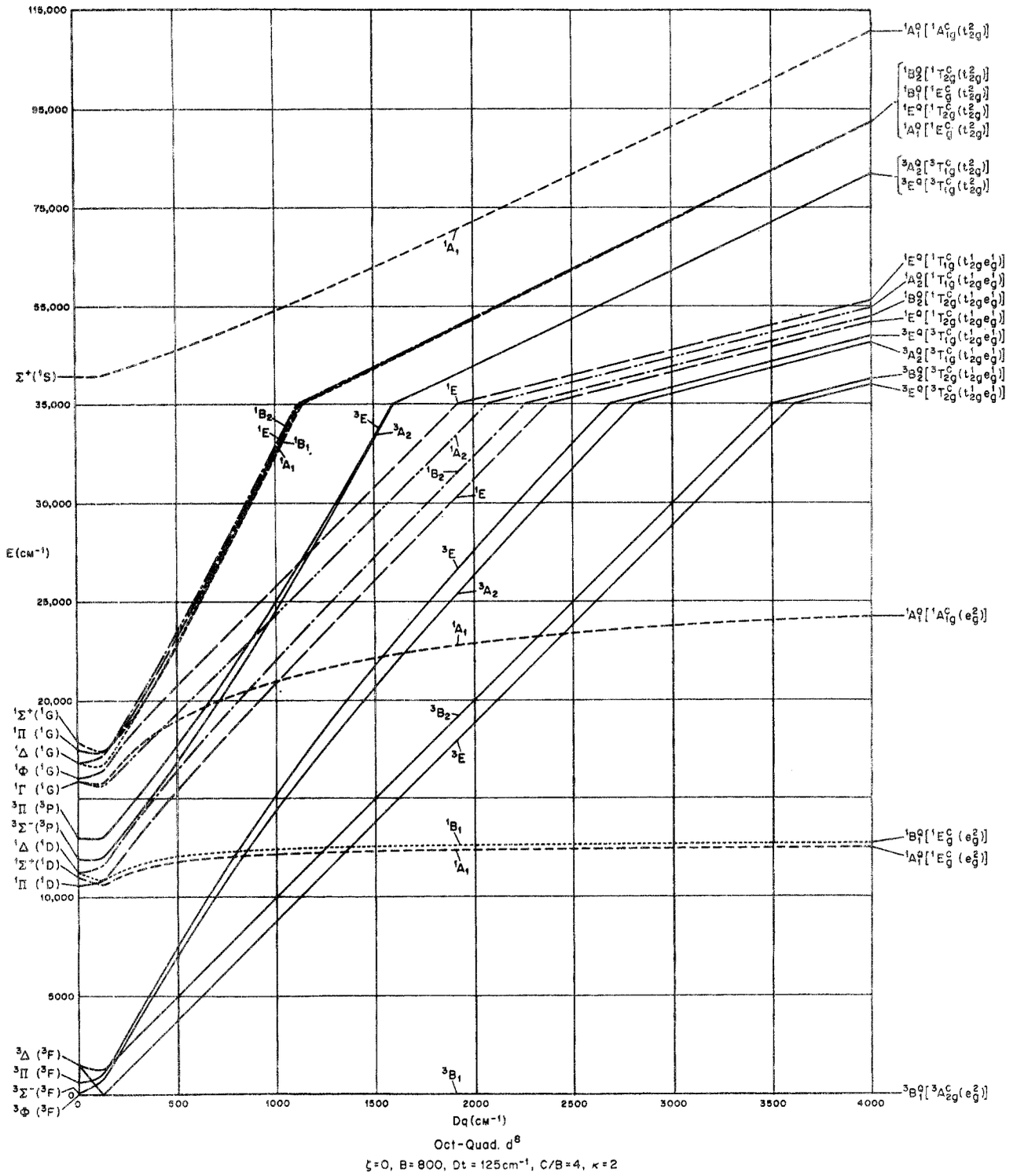

Figure 1. Quadrate splittings of octahedral d^8 energy levels in the limit of zero spin–orbit interaction: $\zeta = 0$, $B = 800$ cm^{-1}, $C/B = 4$, $Dt = 125$ cm^{-1}, $\kappa = 2$.

It is interesting to note that the cubic ^1E level arising from the ground state configuration $t_{2g}^6e_g^2$ does not split in going to quadrate symmetry in the first order, *i.e.*, considering only the diagonal elements. Thus, the energy of both $^1A_1$ and $^1B_1$ quadrate levels of $^1E(e_g^2)$ is given by $12Dq + 7Dt + 2C$ (*cf.* Tables IVa and IVe). It is the configuration interaction that can lift the otherwise degeneracy of this cubic level.[16] The dramatic effect of configuraton interaction in splitting the $^1E(e_g^2)$ cubic level can be seen in Figure 3. The

(16) This situation is exactly similar again to quadrate d^3 systems where also all the cubic (spin) doublets of ground state t_{2g}^3 configuration (^2E_g, $^2T_{1g}$, and $^2T_{2g}$) are split only by configuration interaction in quadrate ligand fields just as the ^2E_g and $^2T_{1g}$ levels themselves are in the parent octahedral ligand fields (*cf.* ref 9b).

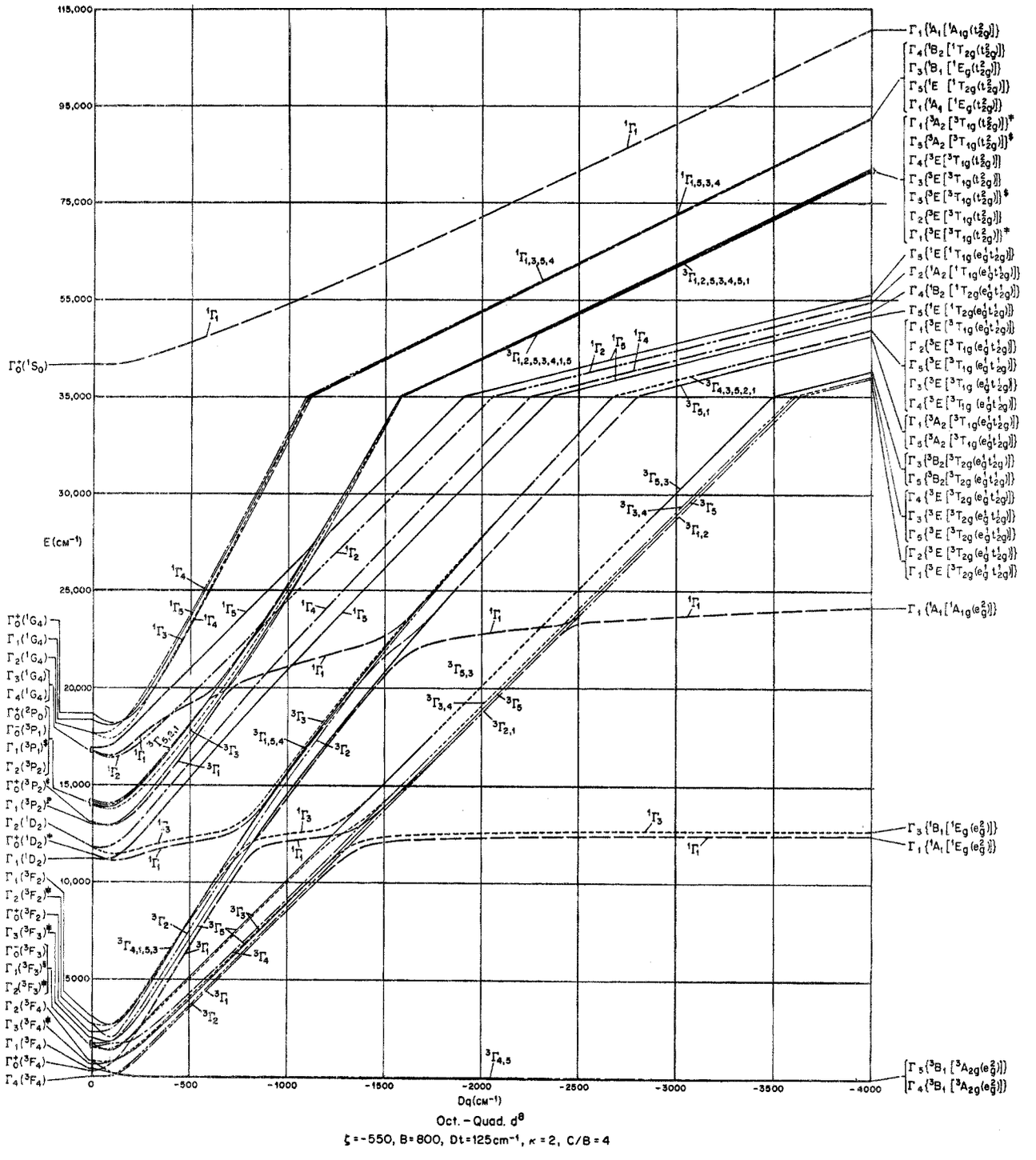

Figure 2. Quadrate splittings of octahedral d^8 energy levels including spin–orbit interaction: $\zeta = -550$ cm^{-1}, $B = 800$ cm^{-1}, $C/B = 4$, $Dt = 125$ cm^{-1}, $\kappa = 2$.

splitting of this level at Dt values appropriate to substituted ammine derivatives ($\sim$350 cm^{-1}) can be as much as $\sim$1500 cm^{-1} and more when spin–orbit coupling is included.[17]

III. Summary

In order to bring out the full significance of complete configuration interaction into focus and for a definitive study of spectral and magnetic properties of quadrate complex compounds of d^2 and d^8 electronic configurations, we have derived the complete energy matrices including spin–orbit perturbation. The symmetry adapted wave functions utilized in the construction of energy matrices have been obtained first in coordinate

(17) J. Merriam and J. R. Perumareddi, to be submitted for publication.

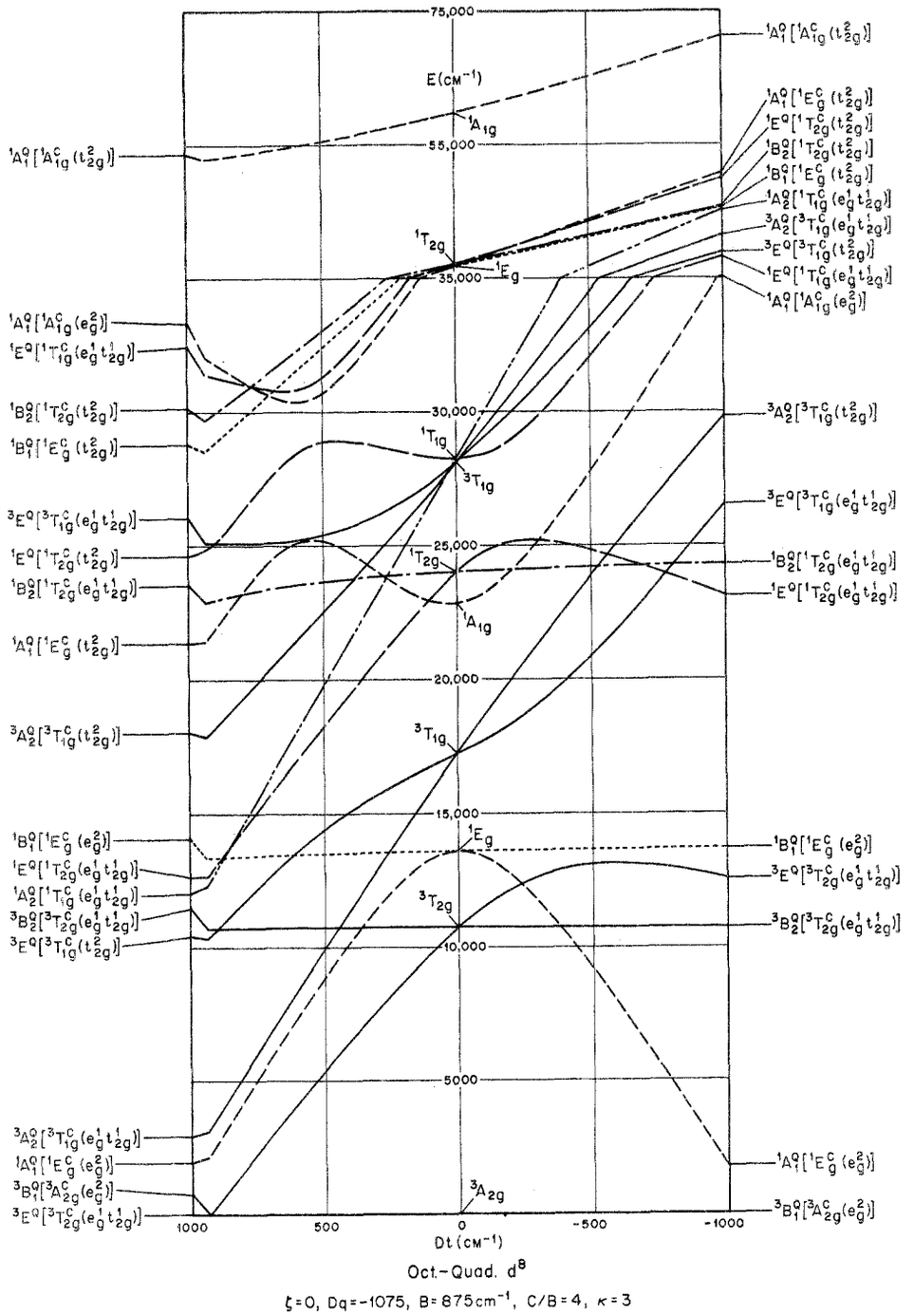

Figure 3. Effect of varying Dt on the quadrate splittings of octahedral d^8 energy levels in the limit of zero spin–orbit interaction: $Dq = 1075$ cm^{-1}, $\zeta = 0$, $B = 875$ cm^{-1}, $C/B = 4$, $\kappa = 3$.

space in strong-field octahedral orientation and then spin oriented so that the quadrate ligand field can be treated as an additive axial ligand field to major cubic ligand field perturbation. The correctness of our secular determinants has been checked by independently calculating all the matrix elements from the energy matrices of other coupling schemes possible for low-symmetry ligand fields and the unitary transformation matrices connecting those coupling schemes with the one used here. Quadrate energy diagrams have been constructed for octahedral d^8 configuration by varying Dq and Dt parameters of the ligand field. These diagrams and similar diagrams that can be obtained for tetrahedral d^8, octahedral and tetrahedral d^2, and for five-coordinate square pyramidal systems of d^2 and d^8 will be utilized in the interpretation of the spectral and other properties of appropriate compounds in subsequent communications.